Numerical Analysis of Convergent-Divergent Angles and Operating Conditions Impact on Rocket Nozzle Performance Parameters

Nabila ALILI*,[1], Khacem KADDOURI[1], Salem MOKADEM[1], Ahmed ALAMI[2]

*Corresponding author
[1]Laboratory of Physical Mechanics of Materials (LMPM),
Mechanical Engineering Department, Djillali Liabes University,
City Larbi Ben Mhidi, P.O. Box 89, 22000 Sidi Bel Abbes, Algeria,
alili.16nabila@gmail.com*, nabila.alili@univ-sba.dz
[2]Laboratory of Process Engineering, Materials and Environment,
Sidi Bel Abbes, Algeria

DOI: 10.13111/2066-8201.2024.16.1.1

Received: 11 January 2024/ Accepted: 05 February 2024/ Published: March 2024

Abstract: *Comprehensive numerical analysis was conducted to elucidate the exhaust performance of rocket engine nozzles. The study focused on unravelling the intricate relationship between convergence and divergence angles and their impact on the exhaust performance parameters, including velocity coefficient (cv), angularity coefficient (Ca), and gross thrust coefficient (Cfg). In contrast to conventional studies that focus mainly on the divergent section, this research delved into both convergent and divergent aspects of nozzle geometry. For the convergent section, a range of angles from 20° to 45° was systematically examined. For the divergent section, a wide spectrum of angles was explored, ranging from small (10°-13°), medium (14°-19°) and large (20°-25°) divergent angles. Further, we venture beyond geometry, investigating the influence of nozzle pressure ratio (NPR) on these key metrics. Realisable $k-\varepsilon$, enhanced wall traitement was used to simulate nozzle flow. The study identified the optimal convergent angle at 37.5°. The 15° diverging angle provides good overall performance, while the 23° angle strikes the ideal compromise: maximizing thrust and efficiency while minimizing weight and maintaining optimal performance.*

Key Words: *Rocket engine nozzle, k-epsilon turbulence model, Convergence angle, Divergence angle, Gross thrust coefficient, Velocity coefficient*

1. INTRODUCTION

Rocket engines are complex systems that require careful design and optimization to achieve optimal performance. One crucial component of a rocket engine is the nozzle, which plays a vital role in converting high-pressure gases into high-velocity exhaust gases. The shape and geometry of the nozzle greatly influence its performance characteristics. These nozzles are specifically configured to achieve supersonic speeds. By passing through the nozzle, the gas pressure and temperature drop, while its velocity increases. The supersonic flow exiting the nozzle possesses immense kinetic energy, which translates into thrust. The choice of the convergent and the divergent angles has a very important impact on the nozzle's efficiency. Several studies and research have been conducted on rocket nozzles, exploring their design,

performance, and optimization. Raghu Ande et al. [1] performed a computational analysis to examine the influence of divergent angle on static pressure and Mach. The study revealed that the divergent angle of 15° yielded the highest Mach number. Ostlund et al. [2] found that a divergent angle of 15° is the best compromise for this type of nozzle. Sunley and Ferriman's [3] investigations into jet separation in conical nozzles revealed that the separation pressure was not consistent and was influenced by the nozzle length. Migdal and Kosson's [4] research focused on predicting shock wave behavior in conical nozzles. They employed the method of characteristics to evaluate pressure and temperature within the nozzle. Paik et al. [5] investigated the relationship between discharge coefficient, flow geometry, and Reynolds number, the study demonstrated a positive correlation between discharge coefficient and mass flow rate. Biju Kuttan P et al. [6] conducted a numerical analysis to determine the optimum divergent angle that would completely eliminate the shock. The results showed that a divergent angle of 15° would completely eliminate the shock and thus would eliminate the shock-induced instabilities. Mason et al. [7] investigated the influence of throat geometry on nozzle flow characteristics, demonstrating the influence of geometry on flow characteristics. Haif S et al. [8] analyze altitude-adapted axisymmetric supersonic nozzles, emphasizing the dual bell nozzle with a central body (DBNCB). Viscous calculations highlight DBNCB's superior performance in different flight phases. The study recommends Fluent code for accurate numerical simulations, offering insights for advancing aerospace propulsion.

Our study aims to analyze the influence of both convergent and divergent angle, alongside with nozzle pressure ratio, on the exhaust nozzle performance parameters for liquid rocket engines. We achieved this by designing and validating a new engine, comparing its performance to the established Merlin 1D. In the first part of our work, we explored a range of convergent angles (25°- 45°) to assess their impact. The second part then delved into divergent angles, categorized into three groups: small (10°-13°), medium (14°-19°), and large (20°-23°). Finally, we investigated the effect of nozzle pressure ratio by analyzing four distinct values (89, 200, 400, and 1000.). Throughout this study, we evaluated the impact of these variations on various crucial exhaust performance parameters, including angularity coefficient, gross thrust coefficient, adiabatic efficiency and velocity coefficient.

2. THE EXHAUST NOZZLE PERFORMANCE PARAMETERS

A set of parameters determines the performance of the exhaust nozzle, that quantify its ability to convert the energy of the hot exhaust gases into thrust. These parameters are investigated in these papers [9], [10].

Gross Thrust Coefficient (C_{fg}) quantifies the efficiency with which the nozzle converts the energy of the exhaust gases into thrust, comparing the actual thrust produced to the theoretical maximum thrust achievable under ideal conditions. A higher C_{fg} indicates more efficient conversion of energy into thrust.

$$F_{\text{actual}} = \dot{m}_{\text{th,actual}} V_e + (P_e - P_a) A_e \tag{1}$$

$$F_{\text{ideal}} = \dot{m}_{\text{th,ideal}} V_s \tag{2}$$

$$C_{fg} = \frac{F_{\text{g ,actual}}}{F_{\text{g ,idel}}} \tag{3}$$

where $\dot{m}_{\text{th,actual}}$ and $\dot{m}_{\text{th,ideal}}$ respectively, represent the actual and ideal mass flow rates through throat. V_e and P_e respectively, represent the velocity and pressure at the nozzle exit. V_s is the Ideal exit velocity. P_a is the ambient pressure, [9], [10].

The nozzle efficiency can be diminished by several factors beyond friction and angularity. Due to the friction between the fluid and the nozzle walls, friction losses occur, leading to a reduction in momentum. Deviations from axial flow at the nozzle's outlet lead to angularity losses, which hinder the effective conversion of exhaust gas energy into thrust. The combined effect of these losses, along with expansion losses, determines the overall efficiency of the nozzle. To account for friction and angularity effects in Equation (1), the gross thrust coefficient can be redefined as follows:

$$C_{fg} = \frac{C_v\, C_a\, \dot{m}_{\text{th,actual}} V_{e,\text{ideal}} + \left(P_{e,\text{ideal}} - P_a\right) A_e}{\dot{m}_{\text{th,actual}} V_s} \tag{4}$$

where C_v is the velocity coefficient. This parameter accounts for the non-ideal conditions within the nozzle, such as friction and turbulence that reduce the actual exit velocity of the exhaust gases compared to the ideal isentropic expansion. A higher C_v indicates less energy loss due to internal friction.

$$C_v = \frac{V_{\text{actual}}}{V_{\text{ideal}}} \tag{5}$$

where:

$$V_{\text{actual}} = \sqrt{RT_{\text{th}(0)}} \sqrt{\frac{2\gamma}{\gamma}\left\{1 - \left(\frac{P_e}{P_{e(0)}}\right)^{\frac{\gamma-1}{\gamma}}\right\}} \tag{6}$$

$$V_{\text{ideal}} = \sqrt{RT_{\text{th}(0)}} \sqrt{\frac{2\gamma}{\gamma}\left\{1 - \left(\frac{P_{e(i)}}{P_{e(0,i)}}\right)^{\frac{\gamma-1}{\gamma}}\right\}} \tag{7}$$

In each expression, $T_{\text{th}(0)}$ is the nozzle throat's stagnation temperature. $P_{e(0)}$ is the exit stagnation pressure. $P_{e(i)}$ is the ideal exit pressure and $P_{e(0,i)}$ is the ideal exit stagnation pressure. R and γ respectively, represent the specific gas constant and the specific heat ratio [9]. The angularity Coefficient (C_a) measures the deviation between the actual and ideal flow directions of exhaust gases. A smaller angularity coefficient optimizes the exhaust flow's uniformity and direction [9].

$$C_a = \frac{\sin\alpha}{\alpha} \tag{8}$$

3. METHODOLGY

3.1 Flow domain

Numerical simulations were employed to simulate the flow behaviour within the 2D convergent-divergent rocket nozzle using ANSYS Workbench R18.1 For this study, a liquid propellant rocket engine was designed utilizing RP-1 and liquid oxygen. The engine was

intended to generate a maximum thrust of 905 kN over a duration of 180 seconds. The combustion chamber was dimensioned to sustain a constant internal pressure of 100 bars. The combustion temperature reached a significant value of 3733 K. The sizing of the combustion chamber and nozzle was determined based on a surface ratio of 13.52. The nozzle's dimensional specifications are detailed in Table 1.

Table 1 – The nozzle dimensions

Convergent length (m)	0.19
Divergent length (m)	1.37
Convergent diameter (m)	0.55
Divergent diameter (m)	1.01
Throat diameter (m)	0.27

To validate the efficiency of our engine design, we opted to compare its performance against the well-established Marlin 1D engine, which is currently in operation. We employed a comparative approach to evaluate the efficiency and performance of our design. The outcomes of this comparison are summarized in Table 2, highlighting key metrics such as specific impulse, maximum thrust, and chamber pressure.

Table 2 – The performance comparison between our designed engine and the Marlin 1D

	Merlin 1D	Our engine
Thrust (KN)	914	905
Specific impulse (s)	311	304.3
Chamber pressure (Bars)	97.2	100
Combustion time (s)	180	180
Mixture ratio	2.34	2.65

3.2 Boundary conditions

We define the study's boundary conditions by specifying internal conditions within the rocket chamber, including a pressure of 100 bar and a temperature of 3730 K and.

The nozzle is designed to optimize performance under ambient conditions, specifically within a temperature range of 300 K and a pressure of 1,013 bar. Nozzle walls adhere to a no-slip condition, maintaining a velocity of zero, and adiabatic considerations are applied to these walls.

It is crucial to highlight that the Combustion parameters are obtained using CEA NASA.

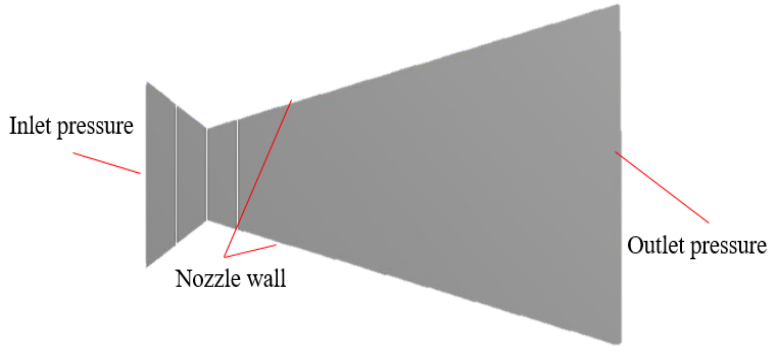

Fig. 1 – Numerical computation domain and boundary conditions

3.3 Mesh generation

The mesh used is of a structured nature in 2D, employing quadrilateral cells, with a maximal concentration of elements in the throat region.

The development of this grid involved a compromise between the result accuracy and the required computation time. A grid refinement study was carefully conducted to optimize both aspects. Fig. 2 provides an enlightening comparison between the predicted static exit pressure distributions using three distinct meshes: Grid A, coarser with 20,702 elements, Grid B, of medium density, with 29,880 elements, and finally, Grid C, finer, totaling 47,121 elements.

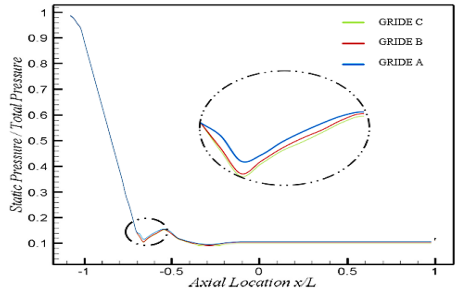

Fig. 2 – Analyzing the forecasted static exit pressure distribution on the nozzle across various grid

Table 3 provides detailed information on the number of nodes and elements for each grid. The comparative analysis reveals that the results obtained with computational grids C and B are extremely similar. Therefore, to optimize the efficiency of the computation process, the decision was made to perform simulations on Grid B, deemed sufficiently accurate while significantly reducing the computation time.

Table 3 – The node and element distribution for f the A, B, and C grids

	Gride A	Gride B	Gride C
Max element size	0.006	0.005	0.004
Number of elements	20702	29880	47121
nodes	62803	90485	142424

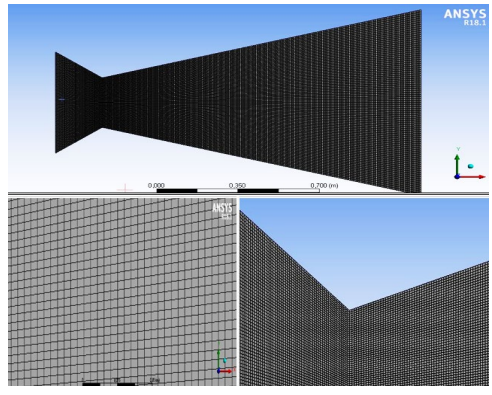

Fig. 3 – The overall overview of computing grids

3.4 The selection of the turbulent model

Choosing the right turbulence model is essential for accurately predicting the behavior of turbulent flows. Several studies have investigated the effectiveness of various turbulence models in different flow scenarios. Kumar Lohia et al. [11] utilized the standard k-ε model in

their study, demonstrating its ability to accurately predict flow parameters and shockwave formation. Launder and Spalding [12]. Examined the k-ε turbulence model's performance in modeling the complex flow characteristics of a jet exiting a convergent-divergent nozzle, finding it to be suitable for the low Reynolds number flows. Dash et al [13]. Evaluated the effectiveness of various two-parameter differential turbulence models in predicting the behavior of expanded supersonic jets. The k-ε realizable and transition SST turbulence models emerged as the most promising candidates. Based on these studies, the Realizable k-ε turbulence model, enhanced wall treatment was selected for this study due to its superior predictive performance.

4. RESULTS AND DISCUSSIONS

4.1 Effect of convergent half- angles (β)

In this part, convergent angles were selected from 25° to 45°. The aim was to analyze how these angles affect the exhaust performance parameters of rocket nozzles. Analysis revealed a sweet spot at 37.5° for optimizing rocket nozzle performance.

This configuration delivered the highest Mach number (3.03) for maximum exhaust velocity (Fig. 4 and Fig. 5), while minimizing static pressure (approaching ambient pressure). Notably, at this angle, the velocity coefficient also peaked at 99.48% (Fig. 6), indicating minimal flow losses.

Furthermore, both gross thrust coefficient (93.08%) and adiabatic efficiency (99.667%) reached their zenith at 37.5° (Fig. 7 and Fig. 8), underscoring the superior performance of this convergent angle across key metrics.

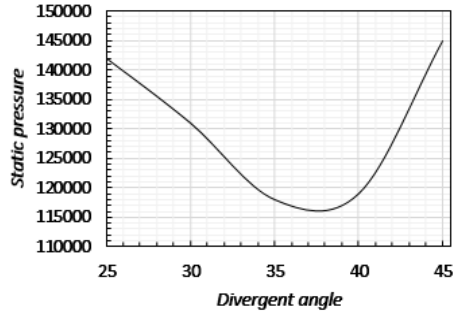

Fig. 4 – Exit static pressure with various convergence angles (β)

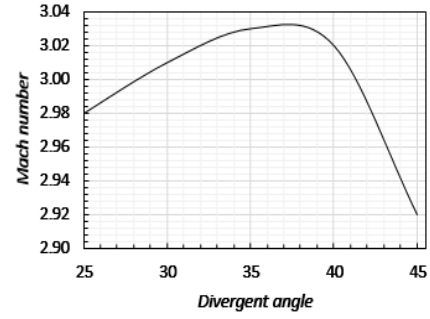

Fig. 5 – Exit Mach number with various convergence angles (β)

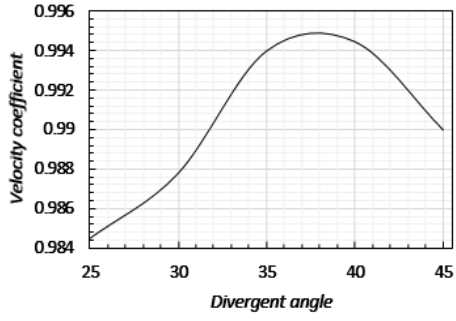

Fig. 6 – Velocity coefficient *(Cv)* with various convergence angles (β)

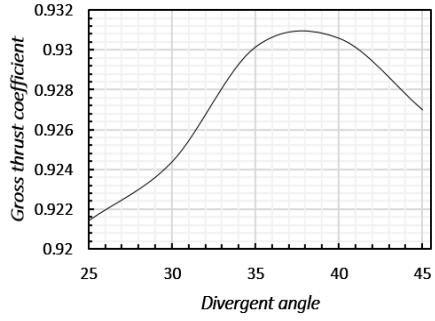

Fig. 7 – Gross thrust coefficient *(Cfg)* with various convergence angles (β)

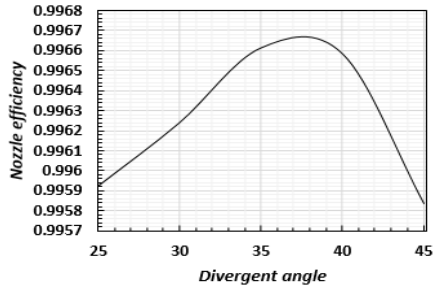

Fig. 8 – Nozzle efficiency (η_n) with various convergence angles (β)

4.2 Effect of divergent half- angles (α)

To investigate the effect of divergent angle on the performance parameters of rocket nozzles, three distinct ranges of divergent angles were selected : Small Range (11° to 14°), Medium Range (15° to 19°), and Large Range (20° to 23°): This range encompasses the largest divergent angles.

4.2.1 Small Range

Simulations revealed that a divergent angle of 11.2 degrees maximized the attainable Mach number (3.02) while concurrently maintaining static pressure of 165,000 Pa. This pressure is slightly higher than the ambient atmospheric pressure. Further investigation into the angularity coefficient (Fig .12) reveals a consistent decrease in *Ca* with increasing the divergent angle. Analysis of the velocity coefficient (Fig. 11) reveals a peak of 96.7% at a divergent angle of 11.2°. Similarly, this angle provides highest gross thrust coefficient (90.95%), and near-perfect adiabatic efficiency (99.53%), indicating minimal energy losses and maximizing propulsive force. However, nozzles with this divergent angle are also longer, with a length of approximately 2.43 meters.

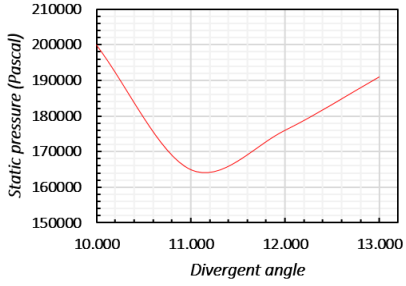

Fig. 9 – Exit Static pressure with various divergence angles (α) 10°-13°

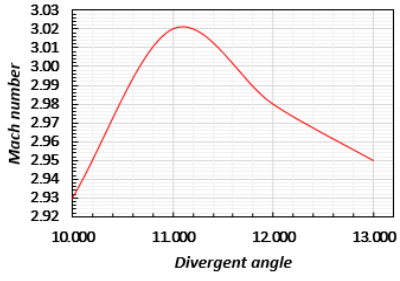

Fig. 10 – Exit Mach number with various divergence angles (α) 10°-13°

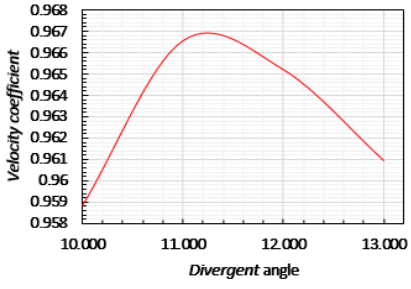

Fig. 11 – Velocity coefficient *(Cv)* with various divergence angles (α) 10°-13°

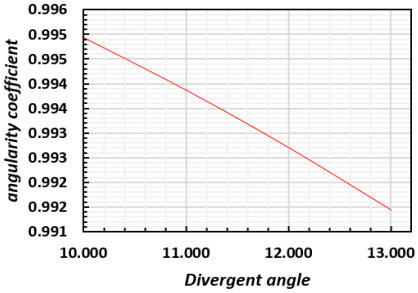

Fig. 12 – Angularity coefficient (Ca) with various divergence angles (α) 10°-13°

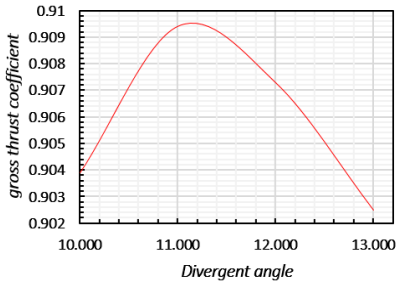

Fig. 13 – Gross thrust coefficient *(Cfg)* with various divergence angles (α) 10°-13°

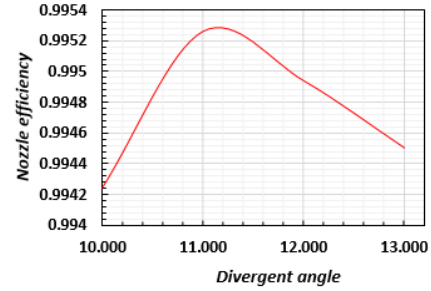

Fig. 14 – Nozzle efficiency (η_n) with various divergence angles (α) 10°-13°

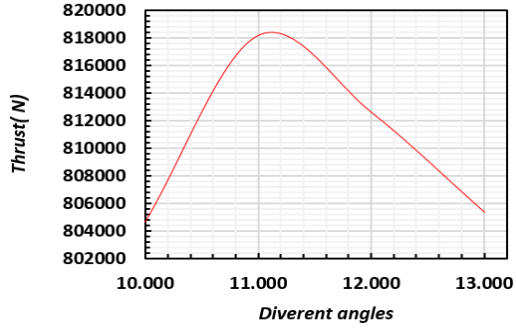

Fig. 15 – Actual thrust with various divergence angles (α) 10°-13°

4.2.2 Medium Range

The findings presented in Figs. 16 and 17 elucidate the influence of the divergent angle on both Mach and pressure. The numerical data reveals an initial rise in Mach number to 3.11 at an angle of 16°, followed by a progressive decline with increasing angle. Conversely, the pressure exhibits a decrease, reaching its minimum value of 118,000 Pa at 15.2°, with an upward observed thereafter. The angularity coefficient exhibits a decreasing trend as the divergent angle increases.

This implies a more gradual expansion of the exhaust gases with widening divergent angles. At a 15° divergent angle, the nozzle reaches its zenith, exhibiting peak performance across all key metrics.

Its velocity coefficient is 99.4%. Similarly, the gross thrust coefficient is 93% and adiabatic efficiency of 99.67%, respectively. Notably, this configuration also delivers the maximum thrust of 837.81 KN, with a compact nozzle length of around 1.9 meters.

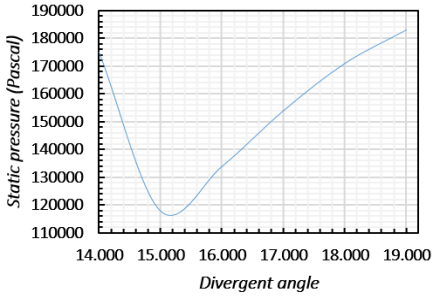

Fig. 16 – Exit static pressure with various divergence angles (α) 14°- 19°

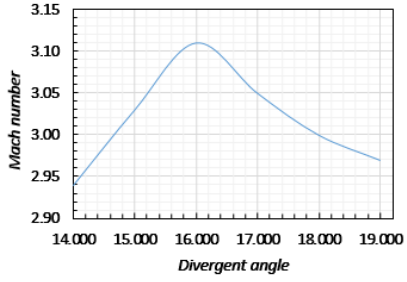

Fig. 17 – Exit Mach number with various divergence angles (α) 14°- 19°

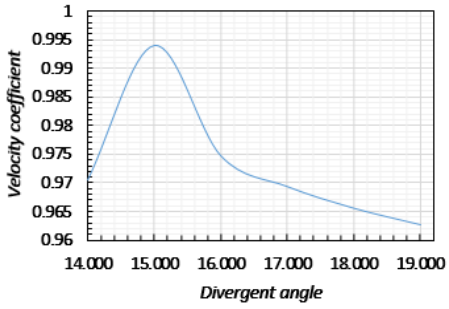

Fig. 18 – Velocity coefficient *(Cv)* with various divergence angles (α) 14°- 19°

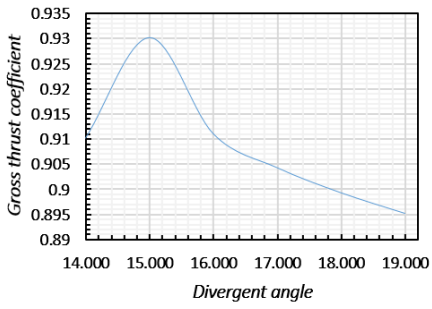

Fig. 19 – Gross thrust coefficient *(Cfg)* with various divergence angles (α) 14°- 19°

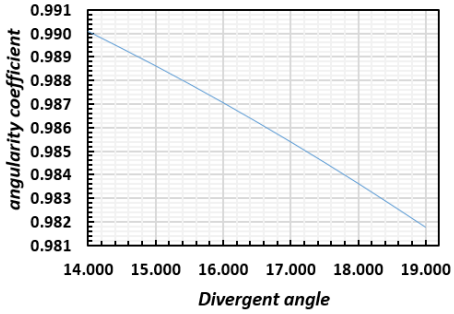

Fig. 20 – Angularity coefficient *(Ca)* with various divergence angles (α) 14°- 19°

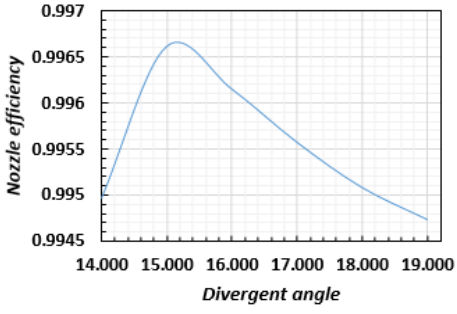

Fig. 21 – Nozzle efficiency *(η_n)* with various divergence angles (α) 14°- 19°

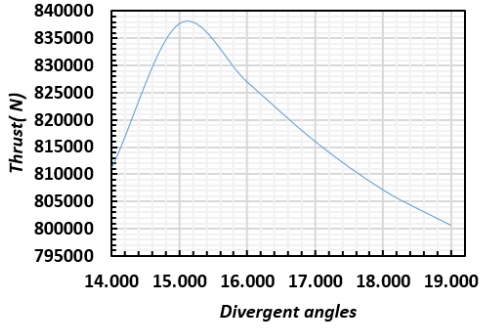

Fig. 22 – Actual thrust with various divergence angles (α) 14°- 19°

4.2.3 Large Range

As shown in Figs. 23 and 24, the divergent angle has a significant impact on both pressure and Mach number. Mach number steadily rises with increasing angle, peaking at 3.29 at 23°, then falls. Conversely, pressure steadily drops with increasing angle, reaching its minimum of 76,300 Pa at 23° and similarly, at a divergent angle of 23°. The velocity coefficient attains its peak value of 99.85%. The maximum value for the gross thrust coefficient is achieved at 93.01%, while the adiabatic efficiency also peaks at 99.79%. This underscores the outstanding efficiency of the nozzle design at this particular angle. The maximum thrust of approximately 849.57 KN was achieved with a divergent angle of 23°. The nozzle with this divergent angle has a length of approximately 1.42 meters. Beyond the 23° angle, shockwaves within the nozzle are completely eliminated; however, the angularity coefficient (*Ca*) decreases significantly.

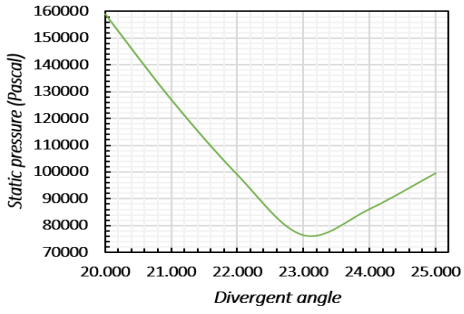

Fig. 23 – Exit static pressure with various divergence angles (α) 20°- 25°

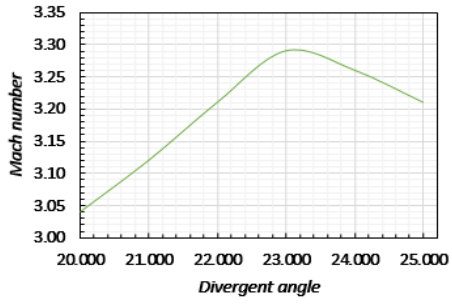

Fig. 24 – Exit Mach number with various divergence angles (α) 20°- 25°

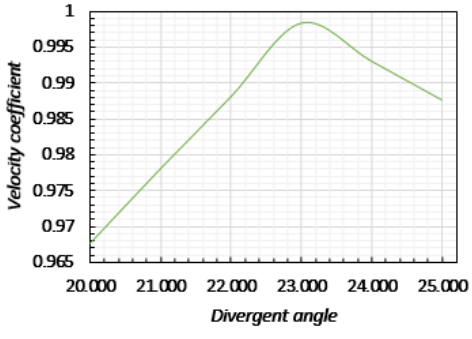

Fig. 25 – Velocity coefficient *(Cv)* with various divergence angles (α) 20°- 25°

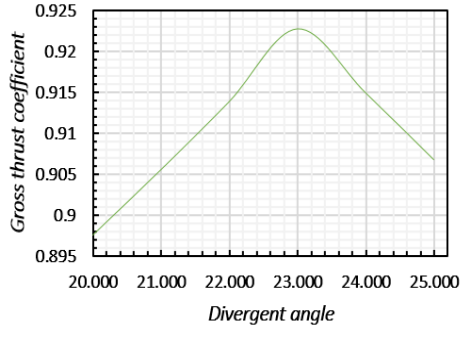

Fig. 26 – Gross thrust coefficient *(Cfg)* with various divergence angles (α) 20°- 25°

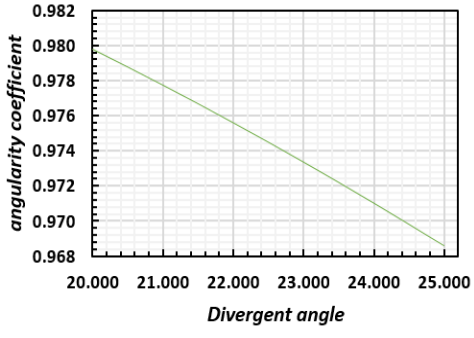

Fig. 27 – Angularity coefficient *(Ca)* with various divergence angles (α) 20°- 25°

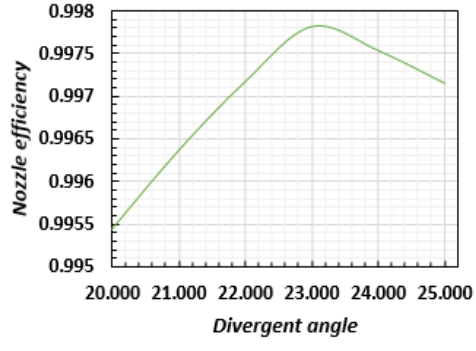

Fig. 28 – Nozzle efficiency (η_n) with various divergence angles (α) 20°- 25°

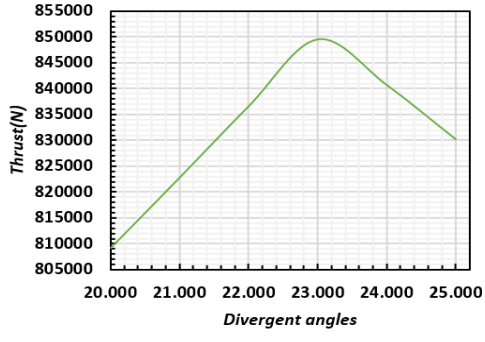

Fig. 29 – Actual thrust with various divergence angles (α) 20°- 25°

4.3 Effect of NPR

To investigate the effect of nozzle pressure ratio (NPR) on exhaust nozzle performance, we conducted numerical simulations for a range of divergent angles (14° to 17°). We chose NPRs of 89, 200, 400, and 1000. The results (Figures 30-32) revealed a consistent trend: increasing the divergence angle by one degree consistently decreased the velocity coefficient (by 1%) and the thrust coefficient (*Cfg*) by 1-2% (except for the 14° angle, which showed a 3% decrease in *Cfg*). Notably, the 15° angle consistently delivered the best performance, with the highest velocity coefficient (99.4%) and the highest *Cfg* (92.3%) at the design NPR of 98. All curves peaked at the design NPR of 98, and increasing NPR beyond that point reduced efficiency for all configurations.

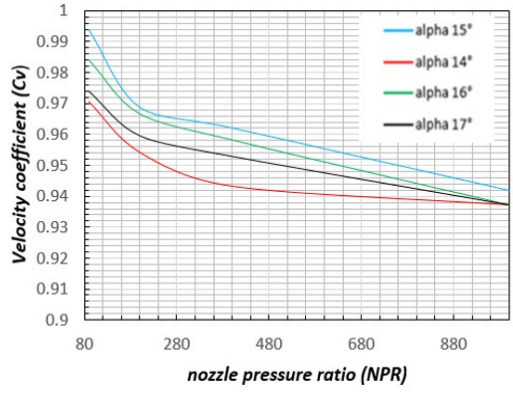

Fig. 30 – Velocity coefficients (*Cv*) across diverse divergence angles at varying nozzle pressure ratios

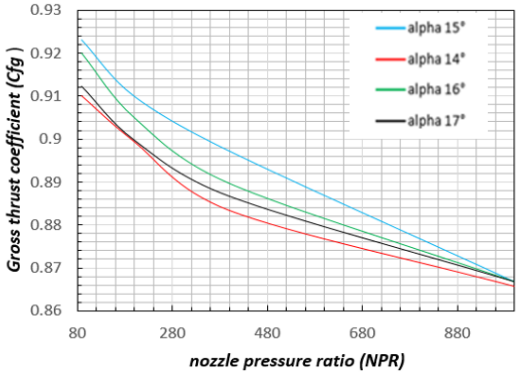

Fig. 31 – Gross thrust coefficient (*Cfg*) across diverse divergence angles at varying nozzle pressure ratios

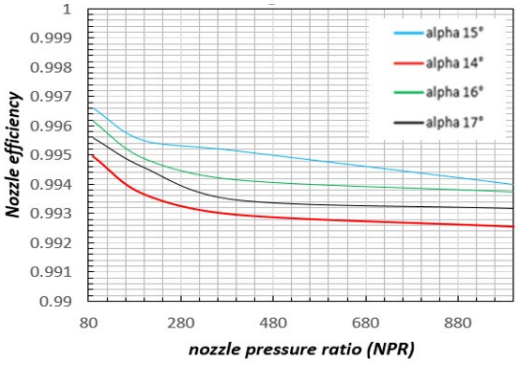

Fig. 32 – Nozzle efficiency across diverse divergence angles at varying nozzle pressure ratios

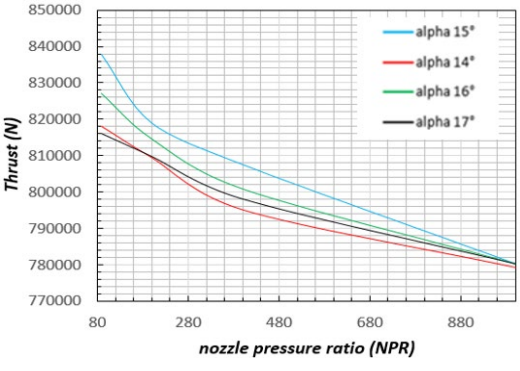

Fig. 33 – Thrust generated across diverse divergence angles at varying nozzle pressure ratios

5. CONCLUSIONS

This study investigated the effect of convergent and divergent angle on the exhaust performance parameters of a designed engine nozzle equivalent to MARLIN 1D engine capable of generating 905 KN thrust. Two-dimensional numerical analyses were conducted to elucidate the optimal configuration for both performance and efficiency.

- The convergent angle of 37.5° was found to be optimal for supersonic nozzles, achieving the highest performance and efficiency.

- for the small range of divergent angle, the 11.2° divergent angle is optimal for maximizing rocket nozzle performances, but it results in a longer and heavier nozzle. This trade-off must be considered during nozzle design.
- The 15° divergent angle provides good overall performance. This is because it balances accelerating exhaust gases to high speeds while maintaining efficiency and minimizing pressure losses.
- The divergent angle of 23° is the optimal for maximizing Mach number, thrust, velocity coefficient, gross thrust coefficient, and adiabatic efficiency while minimizing weight and maintaining optimal performance. However, this large divergent angle comes at the cost of losses due to non-axial flow.
- The NPR of 98 provide the best overall performance, with the highest velocity coefficient, thrust coefficient, and nozzle efficiency. Increasing NPR generally reduces efficiency.

6. REFERENCES

[1] R. Ande and V. N. K. Yerraboina, Numerical investigation on effect of divergent angle in convergent-divergent rocket engine nozzle, *Chemical Engineering Transactions*, vol. **66**, pp. 787–792, 2018, 2283-9216, doi: https://doi.org/10.3303/CET1866132

[2] J. O¨ stlund and B. Muhammad-Klingmann, Supersonic flow separation with application to rocket engine nozzles, *Appl. Mech. Rev.*, vol. **58**, no. 3, pp. 143–177, 2005, 0003-6900, doi: https://doi.org/10.1115/1.1894402

[3] H. L. G. Sunley and V. N. Ferriman, Jet separation in conical nozzles, *The Aeronautical Journal*, vol. **68**, no. 648, pp. 808–817, 1964, 0368-3931, doi: https://doi.org/10.1017/s0368393100081086

[4] D. Migdal and R. Kosson, Shock predictions in conical nozzles, *AIAA Journal*, vol. **3**, no. 8, pp. 1554–1556, 1965, 0001-1452, doi: https://doi.org/10.2514/3.3206

[5] J. S. Paik, K. Am Park, and J. T. Park, Inter-laboratory comparison of sonic nozzles at KRISS, *Flow Measurement and Instrumentation*, vol. **11**, no. 4, pp. 339–344, 2000, 0955-5986, doi: www.elsevier.com/locate/flowmeasinst

[6] P. Biju Kuttan and M. Sajesh, Optimization of divergent angle of a rocket engine nozzle using computational fluid dynamics, *Optimization*, vol. **2**, no. 2, pp. 196–207, 2013, doi: www.theijes.com

[7] M. L. Mason, *The effect of throat contouring on two-dimensional converging-diverging nozzles at static conditions*, National Aeronautics and Space Administration, Scientific and Technical…, 1980.

[8] S. Haif, H. Kbab, and A. Benkhedda, Altitude-compensating axisymmetric supersonic nozzle design and flow analysis, *INCAS Bulletin*, vol. *15*, no. 2, pp. 33–47, 2023, 2066-8201, doi: 10.13111/2066-8201.2023.15.2.4

[9] A. M. Geatz, *A Prediction Code for the Thrust Performance of Two-Dimensional, Non-Axisynnetric, Converging Diverging Nozzles,* 2005, doi: https://scholar.afit.edu/etd/3537

[10] M. H. Hamedi-Estakhrsar, H. Mahdavy-Moghaddam, and M. Jahromi, Investigation of effects of convergence and divergence half-angles on the performance of a nozzle for different operating conditions, *Journal of the Brazilian Society of Mechanical Sciences and Engineering*, vol. **40**, pp. 1–12, 2018, 1678-5878, doi: https://doi.org/10.1007/s40430-018-1271-9

[11] D. K. Lohia and N. Singh, ANALYSIS OF CONVERGENT DIVERGENT NOZZLE WITH RESPECTIVE TO THE POSITION OF FLUID FLOW IN STANDARD AND REALIZABLE TURBULENT MODEL.

[12] D. B. Spalding, The numerical computation of turbulent flow, *Comp. Methods Appl. Mech. Eng.*, vol. **3**, p. 269, 1974, doi: https://doi.org/10.1016/0045-7825(74)90029-2

[13] S. M. Dash, D. C. Kenzakowski, J. M. Seiner, and T. R. S. Bhat, Recent Advances in Jet Flowfield Simulation: Part I–Steady Flows, *AIAA paper*, pp. 93–4390, 1993.